Wiley
Advances in Civil Engineering
Volume 2024, Article ID 3053923, 16 pages
https://doi.org/10.1155/2024/3053923

WILEY

Research Article

A Generalized Limit Equilibrium-Based Platform Incorporating Simplified Bishop, Janbu and Morgenstern–Price Methods for Soil Slope Stability Problems

Aman Alok,[1] **Avijit Burman**,[2] **Pijush Samui**,[2] **Mosbeh R. Kaloop**,[3,4,5] and **Mohamed Eldessouki**[5,6,7]

[1]*Department of Civil Engineering, Indian Institute of Technology Guwahati, Guwahati, India*
[2]*Department of Civil Engineering, National Institute of Technology, Patna, India*
[3]*Department of Civil and Environmental Engineering, Incheon National University, Incheon, Republic of Korea*
[4]*Public Works Engineering Department, Mansoura University, Mansoura, Egypt*
[5]*Digital InnoCent Ltd., London, UK*
[6]*Faculty of Engineering, Mansoura University, Mansoura, Egypt*
[7]*DigInnoCent s.r.o., Liberec, Czech Republic*

Correspondence should be addressed to Mosbeh R. Kaloop; mosbeh@mans.edu.eg

Received 3 March 2023; Revised 15 March 2024; Accepted 29 April 2024; Published 28 May 2024

Academic Editor: Domenico Magisano

Limit equilibrium (LE) method is the most widely used method for slope stability analysis. Different methods based on the LE technique for the analysis of the stability of the slope have been developed. Some are based on satisfying the force equilibrium condition of the failing mass (Janbu's method), while some focus on satisfying the moment equilibrium condition (Bishop's method). Among these methods, the most accurate result is provided by the Morgenstern–Price method as it not only satisfies both moments as well as a force equilibrium condition but also considers the interslice shear forces (V_i) and interslice normal forces (E_i), which are neglected by most of the LE methods to avoid the condition of indeterminacy. To accommodate these forces, Morgenstern–Price (MP) gave a relation between the V_i and E_i which depends upon a scaling multiplier (λ). Thus, it becomes necessary to evaluate λ value along with the factor of safety (*FS*). There is barely any work discussing the detailed methodology of evaluation of λ along with *FS*. Method for obtaining λ along with *FS* have been developed and elaborated in details here. While calculating *FS* (MP method), evaluation of E_i is a must which is dependent upon the values of normal force at the base of each slice (N_i) and *FS*, which itself is dependent upon the value of E_i, making it a loop of interdependent variables. To avoid this interdependency of above stated variables, a separate formulation of E_i is given which reduces the calculations (run-time) involved. A VBA code-based platform has also been developed incorporating the generalized LE method, including Bishop's, Janbu's, and Morgenstern–Price methods which are represented in the form of flowcharts in this work.

1. Introduction

The slope stability analysis primarily focuses on determining a safety index called the factor of safety (*FS*) to identify the critical failure surface (CFS). The *FS* value of any slope against failure can be determined using either the limit equilibrium (LE) method [1, 2, 3, 4], finite element method (FEM)-based strength reduction technique [5, 6, 7, 8], limit analysis method [9, 10, 11, 12, 13], and random limit equilibrium methods (RLEM) [14, 15]. The LE method defines *FS* of any slope as the ratio of the resisting forces/moment trying to stabilize the slope to the driving forces/moment responsible for destabilizing it. One of the major assumptions inherent in LE method-based slope analysis is that the shape of the failure surface is predefined, i.e., circular, logarithmic spiral, piecewise linear, etc. Many probable failure surfaces are investigated, and the failure surface with minimum *FS* value is reported as the CFS.

On the other hand, a strength reduction technique (SRT)-based FEM solution attempts to induce stress failure of the slope, and thus CFS is found when a stress failure has occurred

within a slope domain. SRT does not require any prior assumption regarding the shape of the failure surface, and the failure happens naturally. Limit analysis-based slope analysis investigates a slope based on the upper bound and lower bound theorem while assuming soil as a perfectly plastic material [16, 17, 18, 19]. Here the limiting condition for any slope is obtained by determining the best upper bound value (least) and the best lower bound value (highest) by examining different permissible states of stress [20, 21]. A few of literatures [22, 23, 24, 25] discussed the stability of unsupported rock slopes mostly based on Hoek–Brown model. In some cases, [26, 27, 28] machine learning techniques are involved in slope stability analysis. Though all these methods can be reliably applied for slope stability analysis, the LE method is still used worldwide because of its simplicity and robustness.

In the LE method, the expression of *FS* is formulated by satisfying either moment equilibrium [3], force equilibrium [2], or both [4, 29, 30] for a slice taken from the failure mass and subjected to all internal and external forces. Janbu [2] derived the expression of *FS* by satisfying only the force equilibrium of the failing mass and ignoring interslice shear and normal forces. Bishop's simplified method [3] also ignores interslice shear and normal forces for estimating the *FS*. Bishop and Morgenstern [31] developed a concept of obtaining *FS* for any slope by determining its stability coefficients. Morgenstern and Price [4], on the other hand, proposed a method of calculating *FS* by satisfying both moment and force equilibrium of the failing mass. It is to be noted that the consideration of both normal and forces makes the resulting equation of *FS* indeterminate. Morgenstern and Price [4] considered that the interslice normal and shear forces are related to each other via an interslice force function $f(x)_i$ and a scaling multiplier called lambda (λ), thus resolving the problem of indeterminacy. Spencer [29] assumed a unit value of the force function for any general shape of the failure surface.

Morgenstern and Price [32] gave a numerical approach based on the Newton–Raphson method for solving the equations satisfying the stability of any failure surface. Fredlund and Krahn [33] presented a generalized LE method that combines Janbu [2] method, Bishop [3] method, and Morgenstern and Price [4] method in a single framework. Chen and Morgenstern [34] derived two integral equations satisfying force and moment equilibrium, respectively, and subsequently obtained the result using the Newton–Raphson method. Arai and Tagyo [35] used the conjugate-gradient method to minimize *FS* to search for CFS. Zhu [36] developed equations satisfying interslice force equilibrium and interslice moment equilibrium. The *FS* and λ values are then obtained using an iterative mechanism involving the Newton–Raphson method. Later [37] also proposed a concise and simplified algorithm for computing both scaling parameters λ and *FS* based on the Morgenstern–Price method. Zolfaghari et al. [38] obtained a relation for the resultant interslice forces acting on each slice. Then, with the help of this resulting formulation, moment and horizontal force equilibrium conditions for the whole failing mass are satisfied in order to develop an objective function. The objective function is then minimized using the genetic algorithm (GA) optimization technique to obtain *FS* and λ values. Slope/W (2021), a very popular software for slope stability analysis, has implemented the generalized LE method for carrying out slope analysis and determining CFS. Shiau et al. [39] developed a multivariate regression analysis for 3D slope stability for homogeneous and layered clay.

In the present paper, a detailed discussion of LE technique for solving slope stability problems has been presented. The iterative techniques to analyze slope stability namely Bishop's, Janbu's, and Morgenstern–Price [2, 3, 4] methods have been used in the developed VBA codes. The purpose of using iterative loops in the analysis is to obtain the converged *FS* result thereby avoiding the *FS* obtained directly form the initially assumed values enhancing the accuracy of the analysis. While in this work only circular failure surface is considered for analysis, the primary focus is upon the effects of various (external) parameters upon the stability analysis of homogeneous as well as heterogeneous (layered) [40] soil slope. These parameters include pore water pressure (μ), surcharge loading (q, kN/m^2), horizontal seismic coefficient (k_h), and vertical seismic coefficient (k_v). A comparison of *FS* values when the slope is subjected under such conditions is also drawn here. The methodology for obtaining scaling multiplier (λ) along with *FS* (Morgenstern–Price method [4]) based on Newton-Raphson approach is represented in this literature. Along with this, the time taken to run the VBA code and number of iterations required to obtain the *FS* and λ values when the slope is subjected under such conditions is also highlighted in this work.

2. Methodology

In the present work, three different methods for obtaining *FS* and λ are developed based on the Morgenstern–Price method [4]. The Morgenstern–Price method considers both moment and force equilibrium of the sliding mass while determining *FS* of a slope. Any LE method begins with the assumption that the nature of the failure surface is known a priori. Bishop's [3] method is more suitable for the circular nature of the failure surface. However, Janbu's [2] method and Morgenstern and Price's [4] method can simulate noncircular failure surfaces, i.e., parabolic, logarithmic spiral, piecewise linear, etc. In this case, the VBA code-based MS-Excel spreadsheet platform has been developed considering the circular failure pattern of slope even for Morgenstern and Price's [4] method.

2.1. Determining Critical Failure Surface (CFS). While determining CFS and the associated minimum *FS* of any slope, the effects of surcharge load (q, kN/m^2) and pore-water pressure (μ) over the sliding mass have been considered in this work. The impact of earthquake loading is simulated through equivalent static loading of the amount k_hW in the horizontal direction and k_vW in the vertical direction [41]. The coefficients k_h and k_v are called seismic coefficients acting toward horizontal and vertical directions, respectively. The *FS* of slope against failure is determined using Morgenstern–Price [4] method.

To obtain CFS, a grid-based search method has been adopted, as illustrated in the flowchart shown in Figure 1. In this method, a

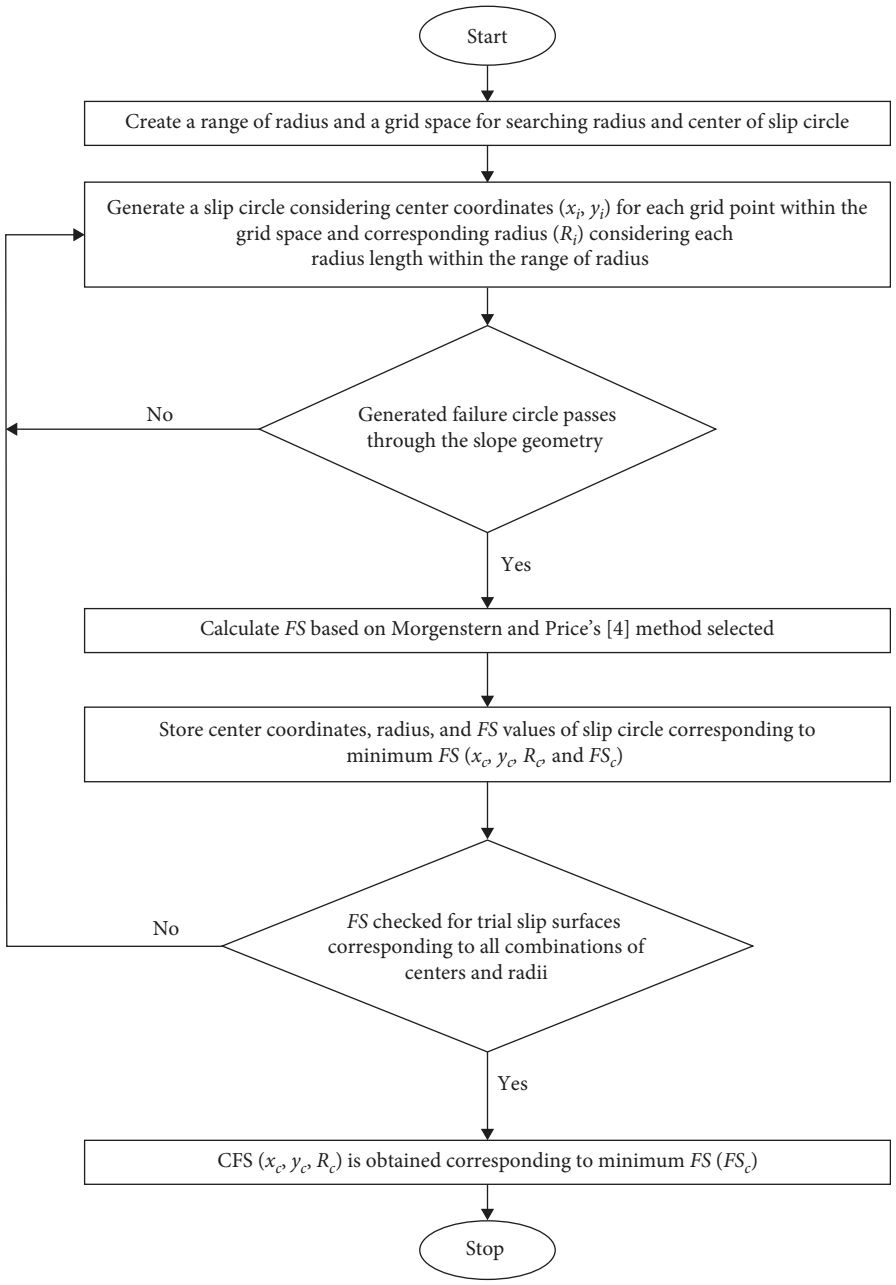

Figure 1: Algorithm for grid-based search method to find out circular CFS.

range for the center (both X and Y coordinates) and radius R of the slip circle is defined. This range is at first divided equally into a predefined number of grid points. Then corresponding to each grid point, a combination of different radius (R) values is used to develop some slip circles. Among all these slip circles, a few slip circles, including those that either do not enter the slope profile or go beyond the base of the slope's foundation, are categorized as invalid circles. The factor of safety FS is determined for all remaining valid slip circles. Finally, the slip circle corresponding to the minimum obtained FS value is called the CFS.

The circular failure mass, which is being considered for the evaluation of FS, is divided into a specified number of slices (n), as represented in Figure 2.

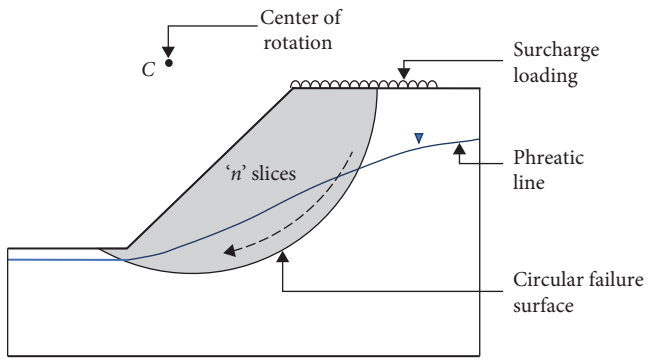

Figure 2: Circular failure surface.

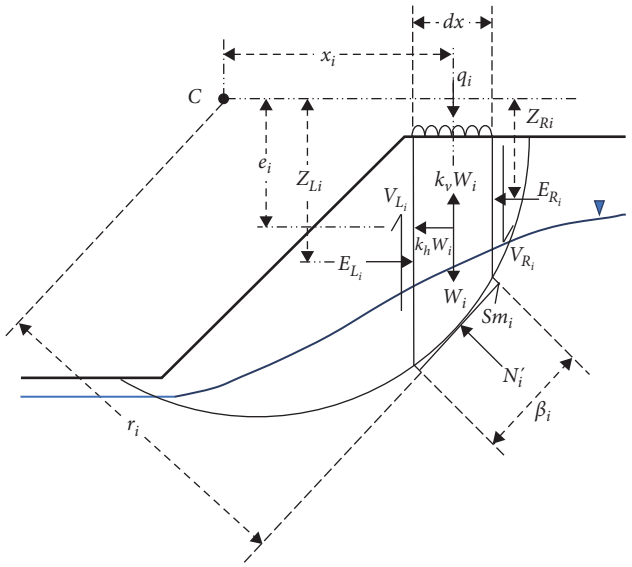

FIGURE 3: Free body diagram of ith slice.

For each slice, all the forces acting on it, along with their respective perpendicular distances from the center of rotation are shown in Figure 3.

All forces on each slice (Figure 3) have been considered for developing an equilibrium equation. In the generalized LE method, horizontal force equilibrium, vertical force equilibrium, and moment equilibrium conditions of each slice and the whole failing mass are considered based on the method being followed.

But when the equilibrium equation is developed while considering all the forces on each slice, its final form becomes indeterminate due to the presence of Interslice normal forces (E_L and E_R) and interslice shear forces (V_L and V_R). So, to avoid this indeterminacy interslice normal forces and interslice shear forces on each slice are neglected in the case of Bishop's simplified method [3] and Janbu's simplified method [2] to calculate FS. But in the case of the Morgenstern and Price's [4] method, both interslice normal and interslice shear forces are considered. To overcome the condition of indeterminacy in the equilibrium equation for calculating FS, Morgenstern and Price considered interslice shear force as a function of interslice normal force for each slice.

Effective normal force (N_i') acting at the base of any *ith* slice having a length of the base β_i is the difference between the normal force (N_i') and the pore water pressure (μ_i) at its base. It can be expressed as given in Equation (1):

$$N_i' = N_i - \mu_i\beta_i. \tag{1}$$

Mobilized shear force at the base of each slice (Sm_i) can be represented as shown in Equation (2):

$$Sm_i = \frac{c_i'\beta_i + N_i' \tan\phi_i'}{FS}, \tag{2}$$

where

$c_i' \longrightarrow$ effective cohesion of the soil layer at the base of ith slice.

$\phi_i' \longrightarrow$ effective angle of internal friction of the soil layer at the base of ith slice.

$FS \longrightarrow$ Factor of safety.

To evaluate the normal force acting on each slice, all the vertical forces on each slice $\sum F_{Vi} = 0$ are balanced, satisfying vertical equilibrium for each slice ith, as shown in Equation (3):

$$V_{Li} - V_{Ri} + Sm_i \sin\alpha_i + N_i\cos\alpha_i - W_i + k_vW_i - q_idx = 0. \tag{3}$$

The normal force acting on each slice is thus obtained, as given in Equation (4):

$$N_i = \frac{V_{Ri} - V_{Li} + W_i - k_vW_i + q_idx - \frac{\left(c_i' - \mu_i \tan\phi_i'\right)\beta_i \sin\alpha_i}{FS}}{\cos\alpha_i + \frac{\tan\phi_i' \sin\alpha_i}{FS}}. \tag{4}$$

If the pore water pressure in the slope is expressed in terms of pore pressure ratio (r_u), the normal force acting on each slice can thus be obtained, as shown in Equation (4a):

$$N_i = \frac{V_{Ri} - V_{Li} + W_i - k_vW_i + q_idx - \frac{\left(c_i' - \frac{W_i r_u}{dx} \tan\phi_i'\right)\beta_i \sin\alpha_i}{FS}}{\cos\alpha_i + \frac{\tan\phi_i' \sin\alpha_i}{FS}}. \tag{4a}$$

2.2. Bishop's [3] Method. As mentioned earlier, Bishop [3] satisfied the moment equilibrium condition for sliding mass $\sum_{i=1}^{n\text{slices}} M_{Ci} = 0$ about its center of rotation (C) for calculating FS, which is given in Equation (5a):

$$\begin{aligned}&\sum_{i=1}^{n\text{slices}} W_ix_i - \sum_{i=1}^{n\text{slices}} k_vW_ix_i + \sum_{i=1}^{n\text{slices}} k_hW_ie_i + \sum_{i=1}^{n\text{slices}} q_ix_i \\ &\quad - \sum_{i=1}^{n\text{slices}} \left(V_{Li}\left(x_i - \frac{dx}{2}\right) - V_{Ri}\left(x_i + \frac{dx}{2}\right)\right) \\ &\quad - \sum_{i=1}^{n\text{slices}} \left(E_{Li}z_{Li} - E_{Ri}z_{Ri}\right) - \sum_{i=1}^{n\text{slices}} Sm_ir_i - \sum_{i=1}^{n\text{slices}} N_if_i = 0.\end{aligned} \tag{5a}$$

The summation of moments developed due to interslice normal forces ($E_{Li}z_{Li}, E_{Ri}z_{Ri}$) and interslice shear forces $[V_{Li}(x_i - \frac{dx}{2}), V_{Ri}(x_i + \frac{dx}{2})]$ on each slice (refer to Figure 3) throughout the failure mass will be zero (Equations (5b) and (5c)) due to the absence of any such external force or moment on the mass:

$$\sum_{i=1}^{n\text{slices}} \left(V_{Li}\left(x_i - \frac{dx}{2}\right) - V_{Ri}\left(x_i + \frac{dx}{2}\right)\right) = 0, \tag{5b}$$

$$\sum_{i=1}^{n\text{slices}} \left(E_{Li}z_{Li} - E_{Ri}z_{Ri}\right) = 0. \tag{5c}$$

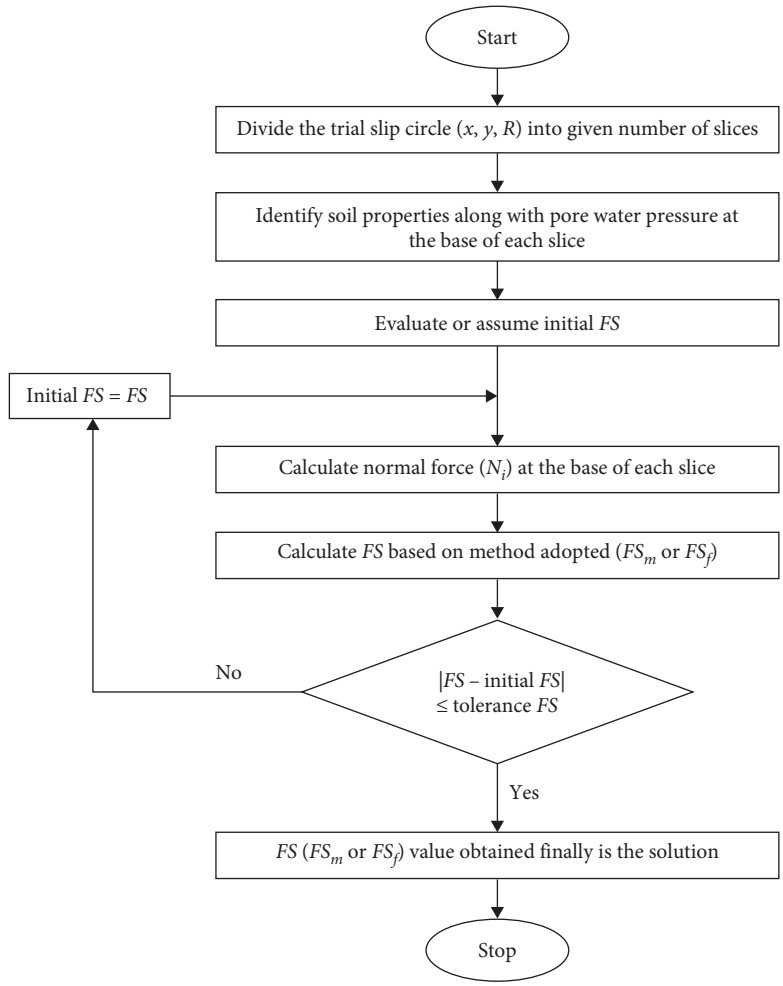

Figure 4: Algorithm to calculate factor of safety (*FS*) based on Bishop and Janbu's method.

Thus, the moment equilibrium equation as obtained in Equation (5a) can be reduced to a simpler form as given in Equation (5d) considering the fact shown in Equations (5b) and (5c):

$$\sum_{i=1}^{n\text{slices}} W_i x_i - \sum_{i=1}^{n\text{slices}} k_v W_i x_i + \sum_{i=1}^{n\text{slices}} k_h W_i e_i + \sum_{i=1}^{n\text{slices}} q_i x_i - \sum_{i=1}^{n\text{slices}} Sm_i r_i - \sum_{i=1}^{n\text{slices}} N_i f_i = 0. \tag{5d}$$

While establishing the moment equilibrium condition, in this case, all clockwise moments about the center of rotation are considered positive moments. In contrast, all anticlockwise moments about the center of rotation are considered negative moments. This equilibrium equation (Equation (5d)) can be rewritten in the form of Equation (6) to obtain moment equilibrium *FS*:

$$FS_m = \frac{\sum_{i=1}^{n\text{slices}} [(c'_i \beta_i + (N_i - \mu_i \beta_i) \tan \phi'_i) r_i]}{\sum_{i=1}^{n\text{slices}} [W_i x_i - k_v W_i x_i + k_h W_i e_i + q_i dx - N_i f_i]}. \tag{6}$$

If the pore water pressure in the slope is given in terms of pore pressure ratio (r_u), the above expression can be represented as shown in Equation (6a):

$$FS_m = \frac{\sum_{i=1}^{n\text{slices}} \left[\left(c'_i \beta_i + \left(N_i - \frac{W_i r_u}{dx} \beta_i \right) \tan \phi'_i \right) r_i \right]}{\sum_{i=1}^{n\text{slices}} [W_i x_i - k_v W_i x_i + k_h W_i e_i + q_i dx - N_i f_i]}. \tag{6a}$$

The computer program developed to determine the *FS* of a given slip circle has been represented as a flowchart shown in Figure 4.

2.3. Janbu's [2] Method. Since Janbu's [2] method for calculating *FS* fulfills the force equilibrium condition for failure mass and satisfaction of vertical force equilibrium has already been factored while calculating normal force at the base of each slice, only fulfillment of horizontal force equilibrium condition $\sum_{i=1}^{n\text{slices}} F_{Hi} = 0$ needs to be considered as represented in Equation (7a):

$$\sum_{i=1}^{n\text{slices}} (E_{Li} - E_{Ri}) + \sum_{i=1}^{n\text{slices}} (Sm_i \cos \alpha_i) - \sum_{i=1}^{n\text{slices}} (N_i \sin \alpha_i) - \sum_{i=1}^{n\text{slices}} (k_h W_i) = 0. \tag{7a}$$

It can be noted that the summation of interslice normal forces (E_{Li}, E_{Ri}) for each slice (refer to Figure 3) throughout the sliding mass will be zero (Equation (7b)) since there is no such external force acting on the mass:

$$\sum_{i=1}^{n\text{slices}} (E_{Li} - E_{Ri}) = 0. \tag{7b}$$

Thus, the horizontal force equilibrium considering the whole failure mass $\sum_{i=1}^{n\text{slices}} F_{Hi} = 0$ obtained in Equation (7a) can be reduced to a more straightforward form, as shown in Equation (7c):

$$\sum_{i=1}^{n\text{slices}} (Sm_i \cos \alpha_i) - \sum_{i=1}^{n\text{slices}} (N_i \sin \alpha_i) - \sum_{i=1}^{n\text{slices}} (k_h W_i) = 0. \tag{7c}$$

To establish a force equilibrium condition, all the forces acting upward and rightward are considered to be acting in a positive direction, while forces acting downward and leftward are considered to be acting in a negative direction. The horizontal force equilibrium equation (Equation (7c)) can be rearranged in the form of Equation (8) to obtain force equilibrium *FS*:

$$FS_f = \frac{\sum_{i=1}^{n\text{slices}} [(c'_i \beta_i + (N_i - \mu_i \beta_i) \tan \phi'_i) \cos \alpha_i]}{\sum_{i=1}^{n\text{slices}} [k_h W_i + N_i \sin \alpha_i]}. \tag{8}$$

The above expression can be rewritten in the form shown in Equation (8a), if the pore water pressure in the slope is given in terms of pore pressure ratio (r_u):

$$FS_f = \frac{\sum_{i=1}^{n\text{slices}} \left[\left(c'_i \beta_i + \left(N_i - \frac{W_i r_u}{dx} \beta_i \right) \tan \phi'_i \right) \cos \alpha_i \right]}{\sum_{i=1}^{n\text{slices}} [k_h W_i + N_i \sin \alpha_i]}. \tag{8a}$$

The flow of the computer program developed to determine the *FS* of a given slip circle has been illustrated in Figure 4.

2.4. Morgenstern and Price's [4] Method. To calculate *FS* by the Morgenstern and Price's [4] method, both force and moment equilibrium conditions must be satisfied for the failure mass taken into consideration. As discussed earlier in this method, interslice normal forces (E_{Li}, E_{Ri}) and interslice shear forces (V_{Li}, V_{Ri}) on each slice (refer to Figure 3) are also considered, and the interslice shear force is expressed in terms of interslice normal forces as represented in Equation (9):

$$V_i = E_i \times \lambda \times f(x)_i \tag{9}$$

where

$\lambda \longrightarrow$ Scaling multiplier.

$f(x)_i \longrightarrow$ Interslice force function for ith slice.

The interslice force function mentioned above can either be considered unity, a constant function, a half sign function, a trapezoidal function, or any other function.

Evaluation of the scaling multiplier (λ) value is a key aspect of the Morgenstern–Price method process, which has not been stated in detail in any work till now. To obtain the value of *FS* along with the scaling multiplier (λ), the Newton–Raphson approach has been used in the present work, all of which have been discussed in detail.

In this case, value of interslice shear forces (V_{Li}, V_{Ri}) acting on the corresponding slice needs to be calculated beforehand to calculate the normal force (Equation (4)) acting at the base of each slice (refer to Figure 3). These interslice shear forces (V_{Li}, V_{Ri}) as per Equation (9) is based on the respective values of interslice normal forces (E_{Li}, E_{Ri}). The horizontal force equilibrium condition for a single slice $\sum F_{Hi} = 0$ can be satisfied, as shown in Equation (10):

$$E_{Li} - E_{Ri} + Sm_i \cos \alpha_i - N_i \sin \alpha_i - k_h W_i = 0. \tag{10}$$

Equation (10), after substituting Equation (2) and Equation (4) in it, can be rewritten in the form of Equation (11) to obtain values of the interslice normal force acting from the right side (E_{Ri}) on each slice.

It is to be noted that calculation procedure of *FS* requires determination of N_i and Sm_i at the base of each slice. For this purpose, the values of N_i and Sm_i should be available beforehand, thus creating a loop of interdependent variables. Earlier, this situation was resolved by assuming an arbitrary value of N_i at first and then calculating the subsequent E_i value. These looped calculations were needed to be repeated multiple times to obtain the desired values of E_i [33].

The expression of interslice normal force acting from right side (E_{Ri}) on each slice is derived in a form which is independent of N_i and Sm_i values, as shown in Equation (11). The presented form is helpful in avoiding repetitive calculation of the abovementioned parameters. After substituting Sm_i from Equation (2) and normal force N_i from Equation (4) into Equation (10), the expression of interslice normal force acting from right side (E_{Ri}) on each slice can be obtained as follows:

$$E_{Ri} = E_{Li} + \frac{(c'_i - \mu_i \tan \phi'_i) \beta_i \sin \alpha_i}{FS} + \frac{V_{Ri} - V_{Li} + W_i - k_v W_i + q_i dx - \frac{(c'_i - \mu_i \tan \phi'_i) \beta_i \sin \alpha_i}{FS}}{FS} \left(\frac{\tan \phi'_i - FS \tan \alpha_i}{\left(1 + \frac{\tan \phi'_i \tan \alpha_i}{FS}\right)^2} \right) - k_h W_i. \tag{11}$$

For the first slice, an interslice normal force acting from the left side is taken as zero ($E_{L1} = 0$) since no external force of such kind is acting on the sliding mass. Substituting this value ($E_{L1} = 0$) in Equation (11) to obtain the interslice normal force on the first slice acting from the right side (E_{R1}). For all other slices ahead, an interslice normal force acting from the left direction ($E_{Li} = 0$) is taken to be equal to the interslice normal force acting from the right direction on the previous slice but in its opposite direction ($E_{Li} = -E_{R(i-1)}$). These values of the interslice normal force acting from the left direction ($E_{Li} = 0$) can be substituted in Equation (11) to obtain corresponding values of the interslice normal force acting from the right direction (E_{Ri}) for all subsequent slices.

In this case, after the E_{Li} and E_{Ri} are obtained, the values of V_{Li} and V_{Ri} acting on the corresponding slice are calculated as represented by Equation (9). These values of V_{Li} and V_{Ri} are substituted in Equation (4) to calculate the value of N_i and Sm_i thus resubstituting these values in Equation (11) repetitively to obtain exact values.

2.5. FS and Scaling Multiplier (λ) Evaluation Using Morgenstern–Price Method. In Morgenstern and Price's [4] method, both moment equilibrium condition (i.e., Equation (5a)), as well as force equilibrium condition (i.e., Equations (3) and (7a)), need to be satisfied and all these expressions directly or indirectly require the calculation of E_{Li} and E_{Ri}. To calculate the E_{Li} and E_{Ri} as given in Equation (11), the value of λ must be known beforehand. In the present work, the Newton–Raphson method has been used to calculate λ along with the *FS*. The detailed procedures of each of these methods are described ahead.

Newton–Raphson method is by far the most widely used methodology of all other root locating methods. In this method, an initial value of the root is to be guessed (x_i say) at first. Then a tangent is extended through the point $[x_i, f(x_i)]$, and the x-intercept of this tangent is noted, corresponding to the improved root estimate. This procedure is repeated to determine a further refined estimate of the root. Thus, we apply the Newton–Raphson technique to evaluate a better-estimated root which is scaling multiplier (λ) in this case for the function given in Equation (12):

$$f_{NR}(\lambda) = FS_m(\lambda) - FS_f(\lambda) = \frac{\sum_{i=1}^{n\text{slices}} [(c'_i\beta_i + (N_i(\lambda) - \mu_i\beta_i)\tan\phi'_i)r_i]}{\sum_{i=1}^{n\text{slices}} [W_i x_i - k_v W_i x_i + k_h W_i e_i + q_i dx - N_i(\lambda) f_i]} - \frac{\sum_{i=1}^{n\text{slices}} [(c'_i\beta_i + (N_i(\lambda) - \mu_i\beta_i)\tan\phi'_i)\cos\alpha_i]}{\sum_{i=1}^{n\text{slices}} [k_h W_i + N_i(\lambda)\sin\alpha_i]}. \tag{12}$$

The root of the above equation can be solved by using the Newton–Raphson method. If the Newton–Raphson method is adopted, the estimate of the root, i.e., scaling multiplier (λ) at $(k+1)$th iteration can be expressed as follows:

$$\lambda_{k+1} = \lambda_k - \frac{f_{NR}(\lambda_k)}{f'_{NR}(\lambda_k)}. \tag{13}$$

For each repetition, along with the value of the governing function $f_{NR}(\lambda)$, the value of its derivative $f'_{NR}(\lambda)$ for the corresponding scaling multiplier (λ) value is needed. This can be calculated from Equation (14a):

$$f'_{NR}(\lambda) = FS'_m(\lambda) - FS'_f(\lambda) = \frac{V_{FS_m}\frac{\partial U_{FS_m}}{\partial\lambda} - U_{FS_m}\frac{\partial V_{FS_m}}{\partial\lambda}}{\left(V_{FS_m}\right)^2} - \frac{V_{FS_f}\frac{\partial U_{FS_f}}{\partial\lambda} - U_{FS_f}\frac{\partial V_{FS_f}}{\partial\lambda}}{\left(V_{FS_f}\right)^2}. \tag{14a}$$

Each term in Equation (14a) can be evaluated based on the expressions given as follows:

$$U_{FS_m} = \sum_{i=1}^{n\text{slices}} [(c'_i\beta_i + (N_i - \mu_i\beta_i)\tan\phi'_i)r_i], \tag{14b}$$

$$V_{FS_m} = \sum_{i=1}^{n\text{slices}} [W_i x_i - k_v W_i x_i + k_h W_i e_i + q_i dx - N_i f_i], \tag{14c}$$

$$\frac{\partial U_{FS_m}}{\partial\lambda} = \frac{(E_{Ri} - E_{Li})\tan\phi'_i f(x)_i r_i}{\cos\alpha_i + \frac{\tan\phi'_i\sin\alpha_i}{FS}}, \tag{14d}$$

$$\frac{\partial V_{FS_m}}{\partial\lambda} = \frac{(E_{Ri} - E_{Li}) f(x)_i f_i}{\cos\alpha_i + \frac{\tan\phi'_i\sin\alpha_i}{FS}}, \tag{14e}$$

$$U_{FS_f} = \sum_{i=1}^{n\text{slices}} [(c'_i\beta_i + (N_i - \mu_i\beta_i))\cos\alpha_i], \tag{14f}$$

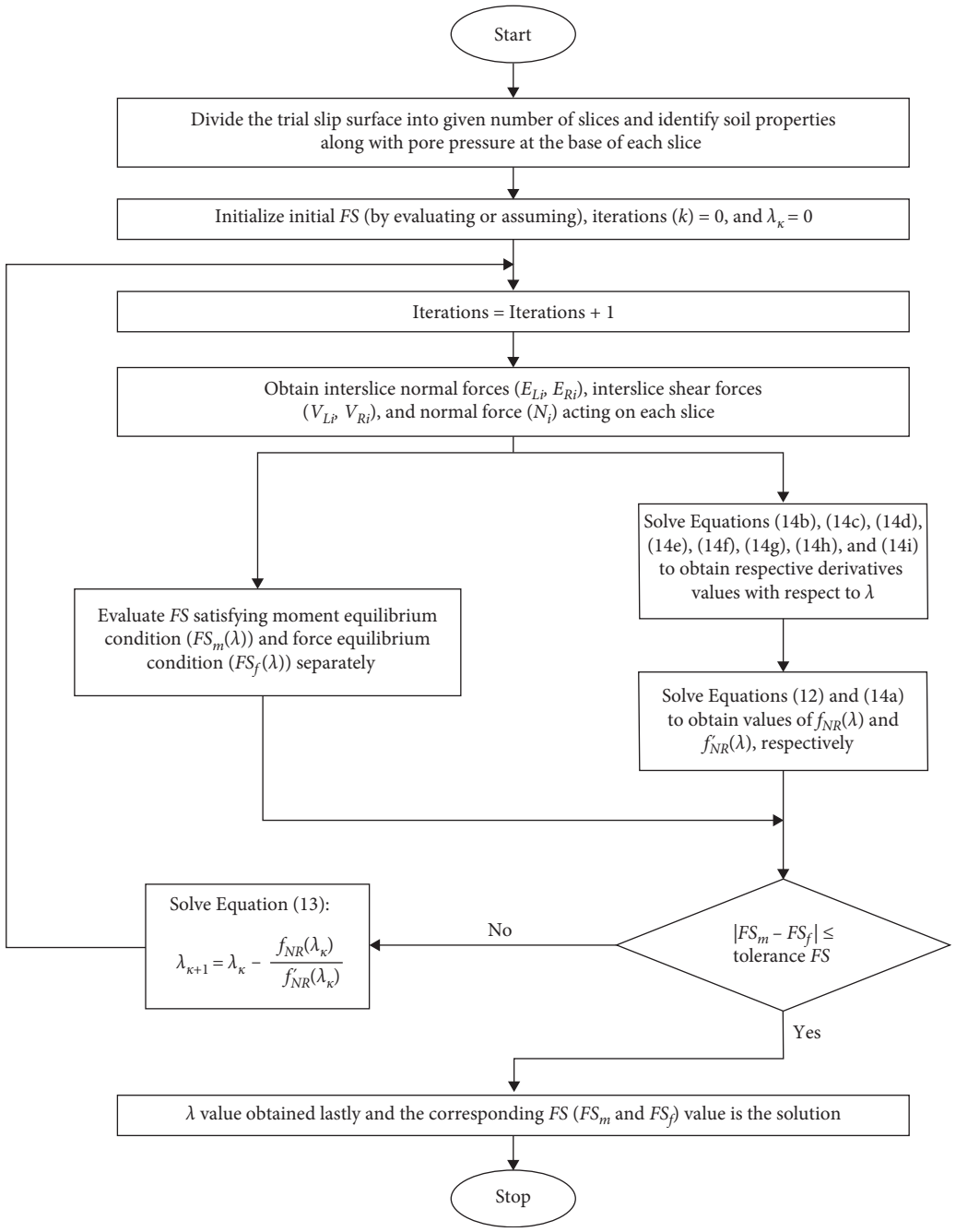

Figure 5: Algorithm to calculate FS (Morgenstern–Price method) and λ by Newton–Raphson method.

$$V_{FS_f} = \sum_{i=1}^{n\text{slices}} [k_h W_i + N_i \sin \alpha_i], \tag{14g}$$

$$\frac{\partial U_{FS_f}}{\partial \lambda} = \frac{(E_{Ri} - E_{Li}) \tan \phi_i' \cos \alpha_i f(x)_i}{\cos \alpha_i + \frac{\tan \phi_i' \sin \alpha_i}{FS}}, \tag{14h}$$

$$\frac{\partial V_{FS_f}}{\partial \lambda} = \frac{(E_{Ri} - E_{Li}) \sin \alpha_i f(x)_i}{\cos \alpha_i + \frac{\tan \phi_i' \sin \alpha_i}{FS}}. \tag{14i}$$

The flowchart of a computer program developed to evaluate the factor of safety (FS) and scaling multiplier (λ) for the Morgenstern–Price method using the Newton–Raphson approach has been shown in Figure 5.

3. Results and Discussion

This section presents slope stability analysis results of a few problems. An MS-Excel spreadsheet platform has been developed incorporating the generalized LE method [2, 3, 4]. Since Morgenstern and Price's [4] method takes into account both interslice normal and shear forces, and as a result, the governing FS determination expression becomes indeterminate. A scaling factor λ is introduced to relate the interslice normal

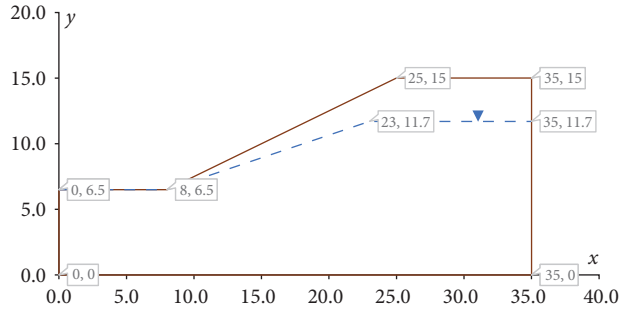

Figure 6: Slope profile for Problem 1.

and shear forces. While applying the Morgenstern–Price method, it is of utmost importance that the scaling multiplier λ should be accurately determined. For this purpose, the present work discusses the Newton–Raphson method. A comparative study has been conducted to assess the efficacy of these methods in their approach to determine *FS*. Either circular or composite type of failure surfaces are considered in the work which stands more accurate for the case of homogeneous soil layer.

Three different problems from existing literature have been chosen here, one of which is a homogeneous soil slope and the other two is a heterogeneous layered soil slope, to test the validation of the developed VBA code-based MS-Excel program and also to check their comparative. Results obtained for both these cases are compared with the results obtained by Zolfaghari et al. [38] for the same problem and illustrated below. The results for specified problems are also being compared with those obtained for the same slope with effects of certain additional conditions such as pore water pressure (μ, kN/m^2), horizontal earthquake coefficient (k_h), vertical earthquake coefficient (k_v), and surcharge loading (q, kN/m^2) applied.

3.1. Problem 1. The first problem, taken from the work of [38] is used to find CFS and minimum *FS* of a homogeneous soil slope having soil properties as follows: effective cohesion $c' = 15$ kN/m^2, the effective angle of internal friction $\phi' = 20°$, and unit weight $\lambda = 19$ kN/m^3. The slope's geometric profile and material properties are depicted in Figure 6. The phreatic surface represented in this figure is considered as reported by Zolfaghari et al. [38]. The slope has been analyzed using a VBA code developed for slope stability analysis using [2, 3, 4].

Grid search limits need to be defined (as represented in Table 1), in which x_i, y_i, x_f, and y_f specify the range to be searched for the center of the critical slip circle while R_i specifying the range of radius to be checked for minimum *FS* at each center point. For this problem, the failure surface is analyzed by dividing it into 50 slices of identical width, and the tolerance limit for obtaining *FS* is kept as low as 0.0001.

As mentioned in grid search input data (Table 1), a grid of coordinates for the center of slip circles is developed, and the minimum *FS* evaluated corresponding to each grid is stored in the corresponding grid location. Finally, the least *FS* among these factors of safeties is printed as the final minimum *FS* along with its corresponding center grid point (i.e., critical center) and radius (i.e., critical radius).

A schematic representation of circular CFS obtained by each of the three methods mentioned, along with each critical

Table 1: Input data for grid search limits (Problem 1).

Grid geometry						
x_i (m)	y_i (m)	x_f (m)	y_f (m)	R_i (m)	R_f (m)	n_{slices}
7	17	17	27	5	25	50

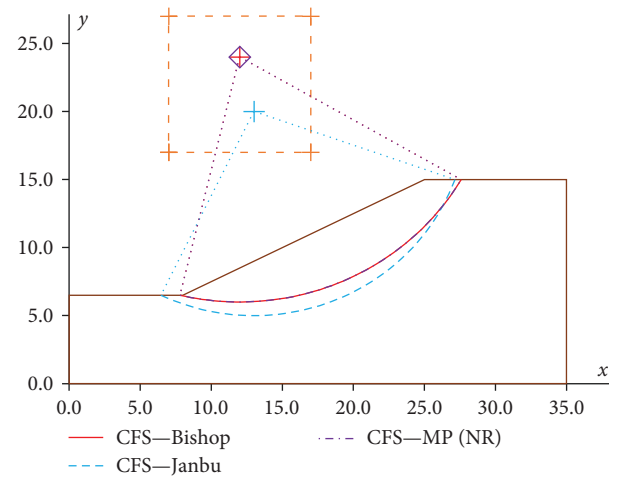

Figure 7: Failure circles obtained for Problem 1 by different methods.

center and center rays, has been depicted in Figure 7. It is observed that all methods yield an almost similar estimation of the center of circular CFS and radius. This shows that the developed program is stable and delivers sufficiently accurate results.

The results obtained are compared with those published by Zolfaghari et al. [38] along with those obtained when pore water pressure (μ, kN/m^2), horizontal earthquake coefficient (k_h), vertical earthquake coefficient (k_v), and surcharge loading (q, kN/m^2) are also applied in Table 2.

For calculation of minimum *FS* and λ by the developed VBA code implementing Newton–Raphson method, the convergence of FS_m and FS_f is studied. FS_m and FS_f are obtained corresponding to all λ values starting from an initial value (i.e., zero) up to a final value λ at which both the factor of safeties become equal (i.e., $FS_m = FS_f$). The convergence of FS_m and FS_f with respect to λ for Newton–Raphson method has been shown in Figure 8. It is observed that the value of $FS = 1.732$ is converged at $\lambda = 0.605$ is obtained using this method.

The *FS* and λ results obtained for the cases when the slope is subjected to pore water pressure loading (μ, kN/m^2) due to considered phreatic surface, as represented in Figure 6, and horizontal earthquake loading of amount k_hW are compared with the result published by Zolfaghari et al. [38]. It is to be noted that [38] only reported the value of the minimum *FS* for this problem but did not mention the value of λ. However, in the present problem, both *FS* and λ have been reported in Table 3. The value of *FS* is seen to match very closely with that reported by Zolfaghari et al. [38]. Here k_h is the horizontal seismic coefficient, whose value is considered 0.1.

Table 4 shows the total run time (T) in seconds and the number of iterations (g) required to run the different VBA program developed for mentioned cases to analyze a given slope. It is seen that when the pore water pressure loadings

Table 2: The values of minimum *FS* obtained for different cases (Problem 1).

Conditions applied for Problem 1		Minimum *FS*		
		Bishop	Janbu	Morgenstern–Price
Zolfaghari et al. [38]	Problem 1	1.74	NA	1.76
VBA program on excel platform	Problem 1	1.742	1.604	1.732
	Problem 1 with μ applied	1.378	1.236	1.370
	Problem 1 with μ and $k_h = 0.1$ applied	1.098	0.970	1.088
	Problem 1 with μ, $k_h = 0.1$, and $k_v = 0.05$ applied	1.093	0.964	1.085
	Problem 1 with μ, $k_h = 0.1$, $k_v = 0.05$, and $q = 5\,\text{kN/m}^2$ applied	1.069	0.941	1.063

μ, pore water pressure. NA, not available.

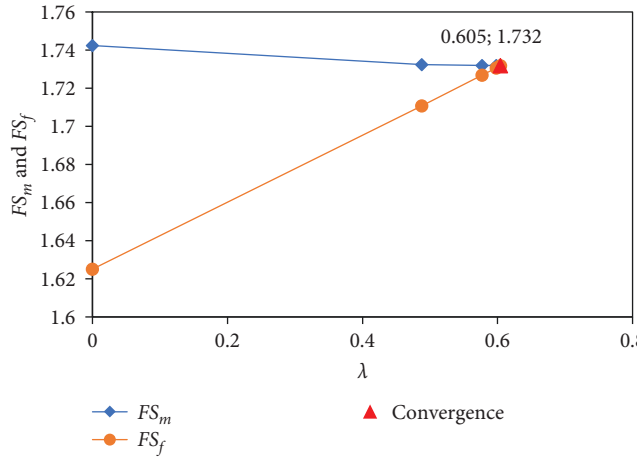

Figure 8: *FS* convergence by Newton–Raphson method (Problem 1).

Table 3: The values of *FS* and λ for different cases (Problem 1).

Conditions applied for Problem 1	Zolfaghari et al. [38]	Morgenstern–Price (Newton–Raphson)	
		Min. *FS*	λ
Problem 1	1.76	1.732	0.605
Problem 1 with μ applied	NA	1.370	0.490
Problem 1 with μ and $k_h = 0.1$ applied	NA	1.088	0.639

NA, not available.

Table 4: Time taken and number of iterations required to run the VBA code for different cases (Problem 1).

Conditions applied for Problem 1	Morgenstern–Price (Newton–Raphson)	
	T (s)	Iterations
Problem 1	10.422	6
Problem 1 with μ applied	10.543	7
Problem 1 with μ and $k_h = 0.1$ applied	10.406	5

are considered, it is observed that the run time and the number of iterations increases very minutely.

3.2. Problem 2. The second problem taken from [38] is to find the critical slip circle and minimum *FS* of a heterogeneous (layered) soil slope having different soil properties for different layers of soil (Figure 9). The geometric profile of the slope along with different material layers are depicted in Figure 9.

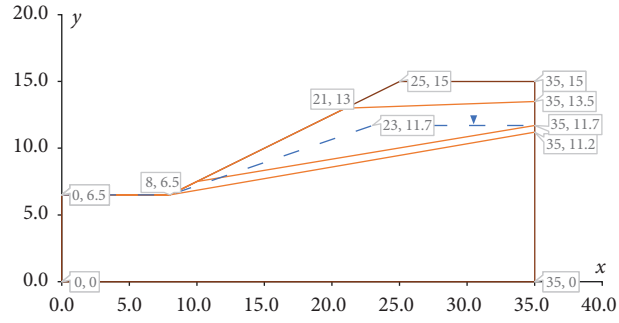

Figure 9: Slope profile for Problem 2.

Table 5: Soil properties of slope considered in Problem 2.

Soil properties	Layer 1	Layer 2	Layer 3	Layer 4
c' (kPa)	15	17	5	35
ϕ'	20°	21°	10°	28°
γ (kN/m^3)	19	19	19	19

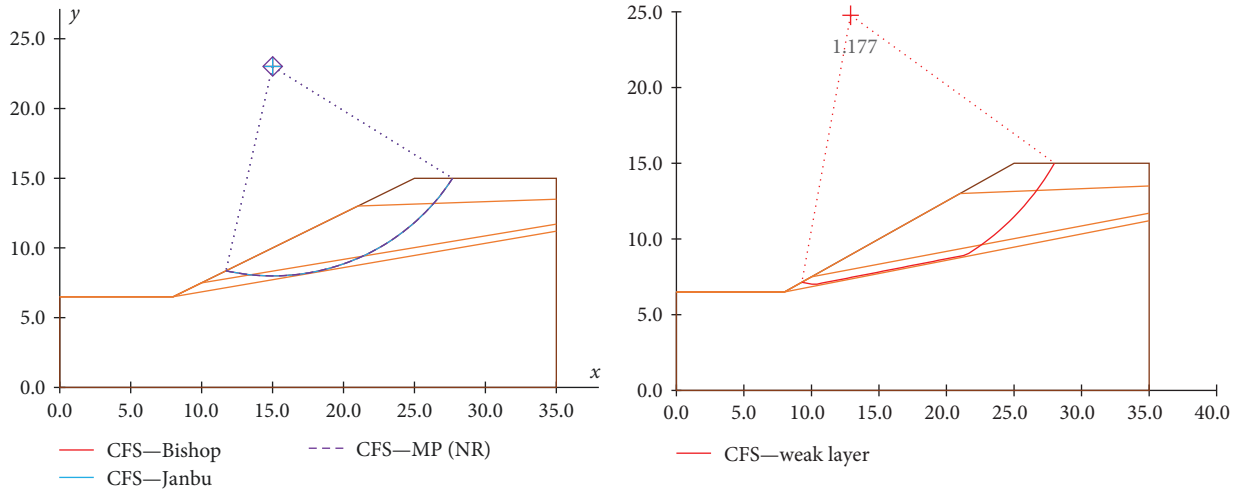

Figure 10: (a) Failure surface obtained for Problem 2 by different methods considering circular slip surface. (b) Failure surface obtained considering composite slip surface.

Table 6: Input data for grid search limits (Problem 2).

Grid geometry						
x_i (m)	y_i (m)	x_f (m)	y_f (m)	R_i (m)	R_f (m)	n_{slices}
7	17	17	27	5	25	50

The slope has been analyzed using a VBA code developed for slope stability analysis using [2, 3, 4].

The soil material properties in each slope layer presented in Figure 9 are shown in Table 5. The slope is also analyzed under the action of pore pressure and earthquake loadings. A phreatic surface, as considered by Zolfaghari et al. [38], is represented in Figure 10. The slope has been analyzed against horizontal earthquake loading k_hW as well as vertical earthquake loading k_vW, where k_h and k_v are horizontal and vertical seismic coefficients, respectively.

The same search grid dimensions, as shown in Table 6, are used for this problem. The failure surface is analyzed by dividing it into 50 slices of equal width, and the tolerance limit for obtaining FS is kept equal to 0.0001. The circular CFS is obtained corresponding to the lowest value of FS found in the entire grid.

A schematic representation of circular CFS obtained by each of the methods mentioned, along with each critical center and center rays, has been depicted in Figure 10(a). It is observed that all methods yield an almost similar estimation of the center of circular CFS and radius. The representation of CFS considering composite pattern of the slip surface has been shown in Figure 10(b), where the failure surface traverses the base of the weak layer. If the failure surface traces the weak layer alignment, the FS value (as per Bishop's simplified method) reduces considerably as the resisting shear strength is predominantly computed considering the weak layer strength parameters. The results are shown in Table 7. The results obtained for this case are verified with the work of [15]. This shows that the developed program is stable and produces sufficiently accurate results.

The results obtained are compared with the result published by Zolfaghari et al. [38] along with the results obtained when pore water pressure (μ, kN/m^2), horizontal earthquake coefficient (k_h), vertical earthquake coefficient (k_v), and surcharge loading (q, kN/m^2) are also applied in Table 7.

When Morgenstern–Price approach is used, the convergence of FS_m and FS_f with respect to λ for Newton–Raphson method has been represented in Figure 11 in the absence of pore pressure and seismic loadings. It is noted that the FS_m and FS_f values finally converge at $\lambda = 0.201$. At this converging point, both FS_m and FS_f values equate to 1.419.

The FS and λ results obtained are further compared with those established by Zolfaghari et al. [38] in Table 8. This table also compares the result evaluated by this method with the additional consideration of pore water pressure loading (μ, kN/m^2) due to phreatic surface, as represented in Figure 11, and horizontal earthquake loading of amount k_hW. Here k_h is the horizontal seismic coefficient, whose value is considered 0.1.

Table 9 shows the total run time (T) in seconds and the number of iterations (g) required to analyze the given slope

Table 7: The values of minimum *FS* obtained for different cases (Problem 2).

Conditions applied for Problem 2		Minimum FS Type of failure surface Circular			Composite
		Bishop	Janbu	Morgenstern–Price	Bishop
Zolfaghari et al. [38]	Problem 2	1.475	NA	1.500	NA
Mafi et al. [15]		NA	NA	NA	1.1
VBA program on excel platform	Problem 2	1.427	1.401	1.419	1.177
	Problem 2 with μ applied	1.289	1.276	1.284	1.024
	Problem 2 with μ and $k_h = 0.1$ applied	1.018	0.998	1.009	0.803
	Problem 2 with μ, $k_h = 0.1$, and $k_v = 0.05$ applied	1.030	1.011	1.021	0.809
	Problem 2 with μ, $k_h = 0.1$, $k_v = 0.05$, and $q = 5\,\text{kN/m}^2$ applied	1.000	0.975	0.989	0.796

NA, not available.

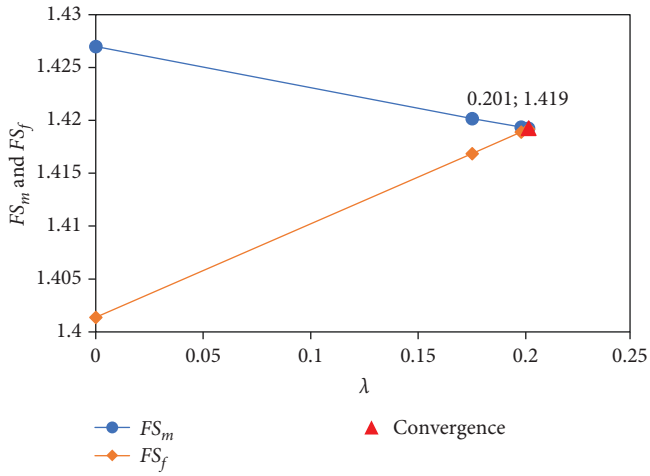

Figure 11: FS convergence by Newton–Raphson method (Problem 2).

Table 8: The values of *FS* and λ for different cases (Problem 2).

Conditions applied for Problem 2	Zolfaghari et al. [38]	Morgenstern–Price (Newton–Raphson)	
		Min. *FS*	λ
Problem 2	1.5	1.419	0.201
Problem 2 with μ applied	NA	1.284	0.103
Problem 2 with μ and $k_h = 0.1$ applied	NA	1.009	0.260

NA, not available.

Table 9: Time taken and number of iterations required to run the VBA code for different cases (Problem 2).

Conditions applied for Problem 2	Morgenstern–Price (Newton–Raphson)	
	T (s)	Iterations
Problem 2	11.825	4
Problem 2 with μ applied	12.344	4
Problem 2 with μ and $k_h = 0.1$ applied	12.015	3

with the help of different VBA program developed for other conditions. It is again observed that the consideration of pore pressure loadings results in a slight increase in the program's run time.

3.3. Problem 3. The third problem taken from [35] is to find the CFS and minimum *FS* of a heterogeneous (layered) soil slope having different soil properties for different layers of soil (Figure 12). The slope has been analyzed using a VBA code developed for slope stability analysis using [2, 3, 4].

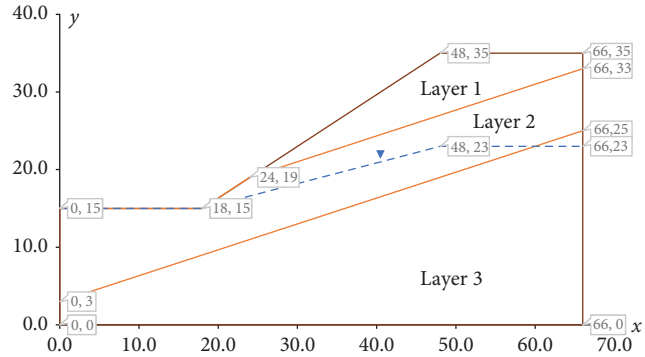

Figure 12: Slope profile for Problem 3.

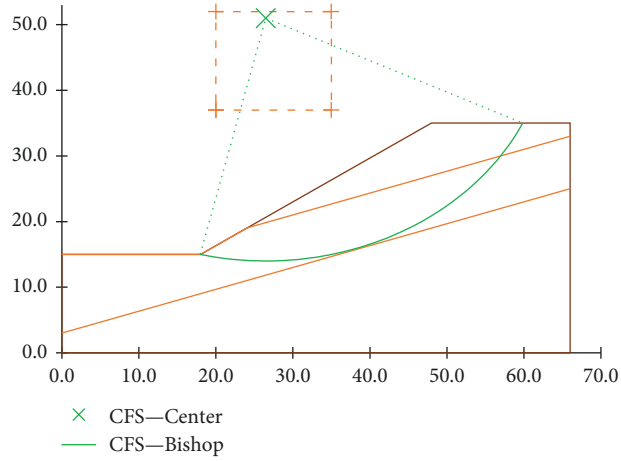

Figure 13: Failure circle obtained for Problem 3 by Bishop's method.

Table 10: Soil properties of slope considered in Problem 3.

Soil properties	Layer 1	Layer 2	Layer 3
c' (kPa)	29.4	9.8	29.4
ϕ'	12°	5°	40°
γ (kN/m^3)	18.82	18.82	18.82

Table 11: Input data for grid search limits (Problem 3).

Grid geometry						
x_i (m)	y_i (m)	x_f (m)	y_f (m)	R_i (m)	R_f	n_{slices}
20	37	35	52	15	45	50

The soil material properties in each slope layer presented in Figure 12 are shown in Table 10. The slope is also analyzed under the action of pore pressure and earthquake loadings. The slope has been analyzed against horizontal earthquake loading k_hW as well as vertical earthquake loading k_vW.

The search grid dimensions, as shown in Table 11, are used for this problem. The failure surface is analyzed by dividing it into 50 slices of equal width, and the tolerance limit for obtaining FS is kept equal to 0.0001. The circular CFS is obtained corresponding to the lowest value of FS found in the entire grid.

A schematic representation of circular CFS obtained by Bishop's method, along with critical center and center rays, has been depicted in Figure 13.

The results obtained are compared with the result published by Arai and Tagyo [35] along with the results obtained when pore water pressure (μ, kN/m^2), horizontal earthquake coefficient (k_h), vertical earthquake coefficient (k_v), and surcharge loading (q, kN/m^2) are also applied in Table 12.

The convergence of FS_m and FS_f with respect to λ for Newton–Raphson method has been represented in Figure 14. It is noted that the FS_m and FS_f values finally converge at $\lambda = 0.199$ to a value of 0.414.

Table 13 compares the FS and λ result evaluated by this method with the additional consideration of pore water pressure loading (μkN/m^2) due to phreatic surface, as represented in Figure 12, and horizontal earthquake loading of amount k_hW (k_h value is considered 0.1).

Table 12: The values of minimum *FS* obtained for different cases (Problem 3).

Conditions applied for Problem 3		Minimum FS		
		Bishop	Janbu	Morgenstern–Price
Arai and Tagyo [35]	Problem 3	0.417	NA	NA
VBA program on excel platform	Problem 3	0.416	0.413	0.414
	Problem 3 considering phreatic surface (μ)	0.380	0.378	0.379
	Problem 3 with μ and $k_h = 0.10$ applied	0.311	0.297	0.309
	Problem 3 with μ, $k_h = 0.1$, and $k_v = 0.05$ applied	0.315	0.302	0.312
	Problem 3 with μ, $k_h = 0.1$, $k_v = 0.05$, and $q = 5\,\text{kN/m}^2$ applied	0.310	0.296	0.306

NA, not available.

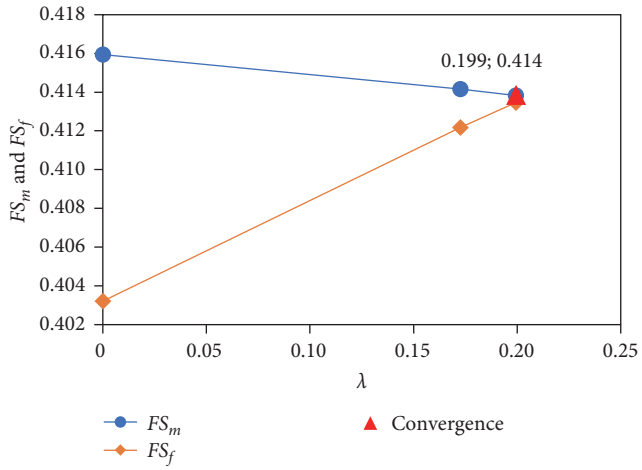

Figure 14: *FS* convergence by Newton–Raphson method (Problem 3).

Table 13: The values of *FS* and λ for different cases (Problem 3).

Conditions applied for Problem 3	Morgenstern–Price (Newton–Raphson)	
	Min. *FS*	λ
Problem 3	0.414	0.199
Problem 3 considering phreatic surface (μ)	0.379	0.117
Problem 3 with μ and $k_h = 0.1$ applied	0.309	0.216

Table 14: Time taken and number of iterations required to run the VBA code for different cases (Problem 3).

Conditions applied for Problem 3	Morgenstern–Price (Newton–Raphson)	
	T (s)	Iterations
Problem 3	17.156	3
Problem 3 considering phreatic surface (μ)	20.108	4
Problem 3 with μ and $k_h = 0.1$ applied	18.918	3

Table 14 compares the total run time (T) in seconds and the number of iterations (g) required to analyze the given slope with the help of different VBA program developed for different conditions. It is again observed that the consideration of pore pressure loadings results in a slight increase in the program's run time.

4. Conclusions

In the current study, for analysis of a given slope, *FS* is being determined based on three different methods following the LE technique, namely Bishop's [3] method, Janbu's [2] method, and Morgenstern and Price's [4] method and a unique formulation for evaluating interslice normal forces (E_i) is given which overcomes the interdependency of normal force (N_i) and the factor of safety (*FS*) and thus reduces the calculations (run-time) involved. The *FS* obtained using these three methods are not only being compared among themselves and the published results of Zolfaghari et al. [38] but also with the results obtained when pore water pressure (μ, kN/m^2), horizontal earthquake coefficient (k_h), vertical earthquake coefficient (k_v), and surcharge loading (q, kN/m^2) are applied. While obtaining CFS in this work, circular trial surfaces are considered based on the grid search technique. Circular failure surfaces are appropriate for analyzing homogeneous soil slope, but for the case of layered (heterogeneous) soil slope composite or generalized failure surfaces are considered. In the current study, circular failure surfaces have been used for most problems. However, for a weak layered soil slope (problem 2), the circular as well as a composite failure surface tracing the alignment of the weak layer have been used. The results obtained are seen to match considerably with the already published results for both cases.

Among the results of *FS* determined using [2, 3, 4], it can be clearly stated that Morgenstern and Price's [4] method gives more accurate results as compared to that evaluated by Janbu [2] and Bishop [3]. This is due to the fact that while Janbu [2] satisfies the force equilibrium condition and Bishop [3] satisfies the moment equilibrium condition [4], method satisfies both conditions for evaluating *FS*. Further, the value of the minimum *FS* obtained by Bishop's method is closer to the minimum *FS* obtained by the Morgenstern–Price method as compared to that obtained by Janbu's method. This is because while evaluating *FS* by Janbu's method, horizontal and vertical force equilibrium conditions are satisfied. Still, to evaluate *FS* by Bishop's method, the moment equilibrium condition is satisfied. For the calculation of normal forces at the base of each slice, the vertical force equilibrium condition for each slice is satisfied. It is also observed that the results of the

minimum *FS* obtained by Bishop's method are quite higher than the value of the minimum *FS* obtained by Janbu's method.

In the present work, the Newton–Raphson technique has been used to determine *FS* and the scaling multiplier λ while analyzing slope stability problems based on Morgenstern and Price's [4] method. Among most methods used in similar problem scenarios, the Newton–Raphson method converges to the result relatively more quickly. It is further observed that the number of steps (iterations) and the run time of the program increases as the effect of pore water pressure and seismic coefficient is taken into consideration.

Abbreviations

W_i: Weight of ith slice
N_i: Normal force at the base of ith slice
Sm_i: Mobilized shear force at the base of ith slice
E_{Li}: Interslice normal force acting on ith slice from left direction
E_{Ri}: Interslice normal force acting on ith slice from right direction
V_{Li}: Interslice shear force acting on ith slice from left direction
V_{Ri}: Interslice shear force acting on ith slice from right direction
q_i: Surcharge load on ith slice in kN/m^2
k_h: Horizontal earthquake coefficient
k_v: Vertical earthquake coefficient
dx: Width of each slice
β_i: Length of base of ith slice
Z_{Li}: Perpendicular distance of E_{Li} from center of rotation
Z_{Ri}: Perpendicular distance of E_{Ri} from center of rotation
x_i: Horizontal distance of center of ith slice from center of rotation
e_i: Vertical distance of center of ith slice from center of rotation
r_i: Perpendicular distance of S_{mi} from center of rotation
f: Perpendicular distance of N_i from center of rotation.

Data Availability

The data used to support the findings of this study are available from the corresponding author upon request.

Conflicts of Interest

The authors declare no conflicts of interest with any other work.

Acknowledgments

This research was supported by Basic Science Research Program through the National Research Foundation of Korea (NRF) funded by the Ministry of Education (GN: NRF-2022R1I1A1A01062918).

References

[1] W. Fellenius, "Calculation of stability of earth dam," in *Proceedings of the Second Congress on Large Dams*, pp. 445–462, Washington, DC, 1936.

[2] N. Janbu, "Application of composite slip surface for stability analysis," in *Proceedings of European Conference on Stability of Earth Slopes*, pp. 43–49, Sweden, 1954.

[3] A. W. Bishop, "The use of the slip circle in the stability analysis of slopes," *Géotechnique*, vol. 5, no. 1, pp. 7–17, 1955.

[4] N. R. Morgenstern and V. E. Price, "The analysis of the stability of general slip surfaces," *Géotechnique*, vol. 15, no. 1, pp. 79–93, 1965.

[5] T. Matsui and K.-C. San, "Finite element slope stability analysis by shear strength reduction technique," *Soils and Foundations*, vol. 32, no. 1, pp. 59–70, 1992.

[6] D. V. Griffiths and P. A. Lane, "Slope stability analysis by finite elements," *Géotechnique*, vol. 49, no. 3, pp. 387–403, 1999.

[7] H. Zheng, D. F. Liu, and C. G. Li, "Slope stability analysis based on elasto-plastic finite element method," *International Journal for Numerical Methods in Engineering*, vol. 64, no. 14, pp. 1871–1888, 2005.

[8] S. Y. Liu, L. T. Shao, and H. J. Li, "Slope stability analysis using the limit equilibrium method and two finite element methods," *Computers and Geotechnics*, vol. 63, pp. 291–298, 2015.

[9] R. L. Michalowski, "Slope stability analysis: a kinematical approach," *Géotechnique*, vol. 45, no. 2, pp. 283–293, 1995.

[10] I. B. Donald and Z. Chen, "Slope stability analysis by the upper bound approach: fundamentals and methods," *Canadian Geotechnical Journal*, vol. 34, no. 6, pp. 853–862, 1997.

[11] C. Viratjandr and R. L. Michalowski, "Limit analysis of submerged slopes subjected to water drawdown," *Canadian Geotechnical Journal*, vol. 43, no. 8, pp. 802–814, 2006.

[12] J. Chen, J.-H. Yin, and C. F. Lee, "Upper bound limit analysis of slope stability using rigid finite elements and nonlinear programming," *Canadian Geotechnical Journal*, vol. 40, no. 4, pp. 742–752, 2003.

[13] J. Chen, J.-H. Yin, and C. F. Lee, "Rigid finite element method for upper bound limit analysis of soil slopes subjected to pore water pressure," *Journal of Engineering Mechanics*, vol. 130, no. 8, pp. 886–893, 2004.

[14] S. Javankhoshdel, B. Cami, R. J. Chenari, and P. Dastpak, "Probabilistic analysis of slopes with linearly increasing undrained shear strength using RLEM approach," *Transportation Infrastructure Geotechnology*, vol. 8, no. 1, pp. 114–141, 2021.

[15] R. Mafi, S. Javankhoshdel, B. Cami, R. J. Chenari, and A. H. Gandomi, "Surface altering optimisation in slope stability analysis with non-circular failure for random limit equilibrium method," *Georisk: Assessment and Management of Risk for Engineered Systems and Geohazards*, vol. 15, no. 4, pp. 260–286, 2021.

[16] D. C. Drucker, W. Prager, and H. J. Greenberg, "Extended limit design theorems for continuous media," *Quarterly of Applied Mathematics*, vol. 9, no. 4, pp. 381–389, 1952.

[17] W. Chen, *Limit Analysis and Soil Plasticity Elsevier*, Science Publishers, Amsterdam, 1975.

[18] W.-F. Chen and X. L. Liu, *Limit Analysis in Soil Mechanics*, Elsevier, 2012.

[19] V. Q. Lai, D. K. Nguyen, R. Banyong, and S. Keawsawasvong, "Limit analysis solutions for stability factor of unsupported conical slopes in clays with heterogeneity and anisotropy," *International Journal of Computational Materials Science and Engineering*, vol. 11, no. 1, Article ID 2150030, 2022.

[20] H. S. Yu, R. Salgado, S. W. Sloan, and J. M. Kim, "Limit analysis versus limit equilibrium for slope stability," *Journal of Geotechnical and Geoenvironmental Engineering*, vol. 124, no. 1, pp. 1–11, 1998.

[21] B. Leshchinsky and S. Ambauen, "Limit equilibrium and limit analysis: comparison of benchmark slope stability problems," *Journal of Geotechnical and Geoenvironmental Engineering*, vol. 141, no. 10, Article ID 04015043, 2015.

[22] W. Yodsomjai, S. Keawsawasvong, and S. Likitlersuang, "Stability of unsupported conical slopes in Hoek–Brown rock masses," *Transportation Infrastructure Geotechnology*, vol. 8, no. 2, pp. 279–295, 2021.

[23] M. Azarafza, M. H. Bonab, and R. Derakhshani, "A novel empirical classification method for weak rock slope stability analysis," *Scientific Reports*, vol. 12, no. 1, Article ID 14744, 2022.

[24] M. Azarafza, H. Akgün, A. Ghazifard, E. Asghari-Kaljahi, J. Rahnamarad, and R. Derakhshani, "Discontinuous rock slope stability analysis by limit equilibrium approaches—a review," *International Journal of Digital Earth*, vol. 14, no. 12, pp. 1918–1941, 2021.

[25] Y. Mao, L. Chen, Y. A. Nanehkaran, M. Azarafza, and R. Derakhshani, "Fuzzy-based intelligent model for rapid rock slope stability analysis using Qslope," *Water*, vol. 15, no. 16, Article ID 2949, 2023.

[26] Y. A. Nanehkaran, T. Pusatli, J. Chengyong et al., "Application of machine learning techniques for the estimation of the safety factor in slope stability analysis," *Water*, vol. 14, no. 22, Article ID 3743, 2022.

[27] Y. A. Nanehkaran, Z. Licai, J. Chengyong et al., "Comparative analysis for slope stability by using machine learning methods," *Applied Sciences*, vol. 13, no. 3, Article ID 1555, 2023.

[28] M. Azarafza, M. H. Bonab, and R. Derakhshani, "A deep learning method for the prediction of the index mechanical properties and strength parameters of marlstone," *Materials*, vol. 15, no. 19, Article ID 6899, 2022.

[29] E. Spencer, "A method of analysis of the stability of embankments assuming parallel inter-slice forces," *Geotechnique*, vol. 17, no. 1, pp. 11–26, 1967.

[30] Z. Fan, H. Tang, Y. Yang, Y. Zheng, Q. Tan, and T. Wen, "Extension of Spencer's circular model to stability analysis of landslides with multicircular slip surfaces," *Mathematical Problems in Engineering*, vol. 2020, Article ID 1298912, 22 pages, 2020.

[31] A. W. Bishop and N. Morgenstern, "Stability coefficients for earth slopes," *Géotechnique*, vol. 10, no. 4, pp. 129–153, 1960.

[32] N. R. Morgenstern and V. E. Price, "A numerical method for solving the equations of stability of general slip surfaces," *The Computer Journal*, vol. 9, no. 4, pp. 388–393, 1967.

[33] D. G. Fredlund and J. Krahn, "Comparison of slope stability methods of analysis," *Canadian Geotechnical Journal*, vol. 14, no. 3, pp. 429–439, 1977.

[34] Z.-Y. Chen and N. R. Morgenstern, "Extensions to the generalized method of slices for stability analysis," *Canadian Geotechnical Journal*, vol. 20, no. 1, pp. 104–119, 1983.

[35] K. Arai and K. Tagyo, "Determination of noncircular slip surface giving the minimum factor of safety in slope stability analysis," *Soils and Foundations*, vol. 25, no. 1, pp. 43–51, 1985.

[36] D.-Y. Zhu, "A method for locating critical slip surfaces in slope stability analysis," *Canadian Geotechnical Journal*, vol. 38, no. 2, pp. 328–337, 2001.

[37] D. Y. Zhu, C. F. Lee, Q. H. Qian, and G. R. Chen, "A concise algorithm for computing the factor of safety using the Morgenstern Price method," *Canadian Geotechnical Journal*, vol. 42, no. 1, pp. 272–278, 2005.

[38] A. R. Zolfaghari, A. C. Heath, and P. F. McCombie, "Simple genetic algorithm search for critical non-circular failure surface in slope stability analysis," *Computers and Geotechnics*, vol. 32, no. 3, pp. 139–152, 2005.

[39] J. Shiau, V. Q. Lai, and S. Keawsawasvong, "Multivariate adaptive regression splines analysis for 3D slope stability in anisotropic and heterogenous clay," *Journal of Rock Mechanics and Geotechnical Engineering*, vol. 15, no. 4, pp. 1052–1064, 2023.

[40] W. Yodsomjai, S. Keawsawasvong, C. Thongchom, and J. Lawongkerd, "Undrained stability of unsupported conical slopes in two-layered clays," *Innovative Infrastructure Solutions*, vol. 6, no. 1, pp. 1–17, 2021.

[41] P. P. Sahoo and S. K. Shukla, "Effect of vertical seismic coefficient on cohesive-frictional soil slope under generalised seismic conditions," *International Journal of Geotechnical Engineering*, vol. 15, no. 1, pp. 107–119, 2021.